Supplemental Materials for

The Role of Phosphate in Silk Fibroin Self-Assembly: A Hofmeister Study

*Caleb Wigham,[1,2] Vrushali Varude,[1,2] Henry O'Donnell,[1] R. Helen Zha[1,2]**

[1]Department of Chemical and Biological Engineering, Rensselaer Polytechnic Institute, Troy, NY 12180

[2]Center for Biotechnology and Interdisciplinary Studies, Rensselaer Polytechnic Institute, Troy, NY, 12180

To quantify the continuous accumulation of silk fibroin at the solid-liquid interface, we fit our two-stage interfacial assembly model developed from previous work[1]. The full derivation, assumptions, and justifications can be found in our prior work.

$$\frac{dM}{dt} = \frac{k_a c^* \left(1 - \frac{M}{M_{max}}\right)}{e^{\beta t}} + k_{ss} \tag{S1}$$

Where dM/dt represents the change in specific mass with respect to time (ng/cm^2/s), M represents specific mass deposition (ng/cm^2) on the surface at time t (s), C* is the effective concentration of the bulk protein solution above the surface (mM), M_{max} is a free-fit parameter representing the maximum mass deposited on the surface (ng/cm^2), β is a fitted time constant (s^{-1}), K_a is the early stage adsorption rate constant (ng/cm^2/s/mM), and k_{ss} is the late stage adsorption rate constant (ng/cm^2/s). In order to directly compare the early and late stage adsorption rate constants, we consider the full term $k_a c^*$ as the early stage adsorption rate constant with units of (ng/cm^2/s). The model fits and residuals for reported adsorption rates constants in the main text are found in **Figures S5 – S8**.

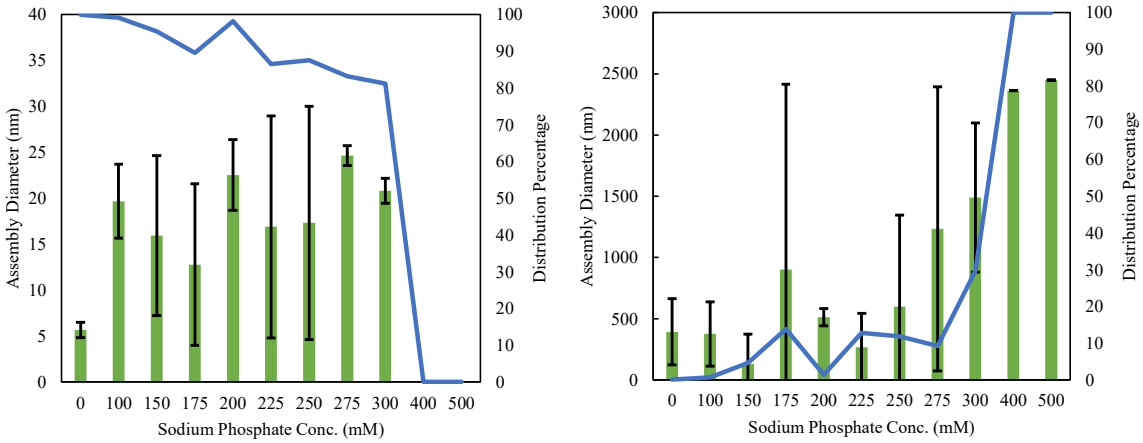

Figure S1: Silk fibroin solution-phase assembly diameters measured by DLS in various concentrations of sodium phosphate at solution pH 5 and silk fibroin concentration of 0.5 mg/mL. Sodium phosphate promotes two distinct populations of silk fibroin assemblies in solution; assembly diameter is shown as green bars and distribution percentage is shown by the blue line. (Left) Small, active assemblies that participate in coating formation. (Right) Large, inactive aggregates that do not participate in coating formation. Assembly diameters are reported as the mean (n = 4) of the distribution and the error bars represent standard deviation.

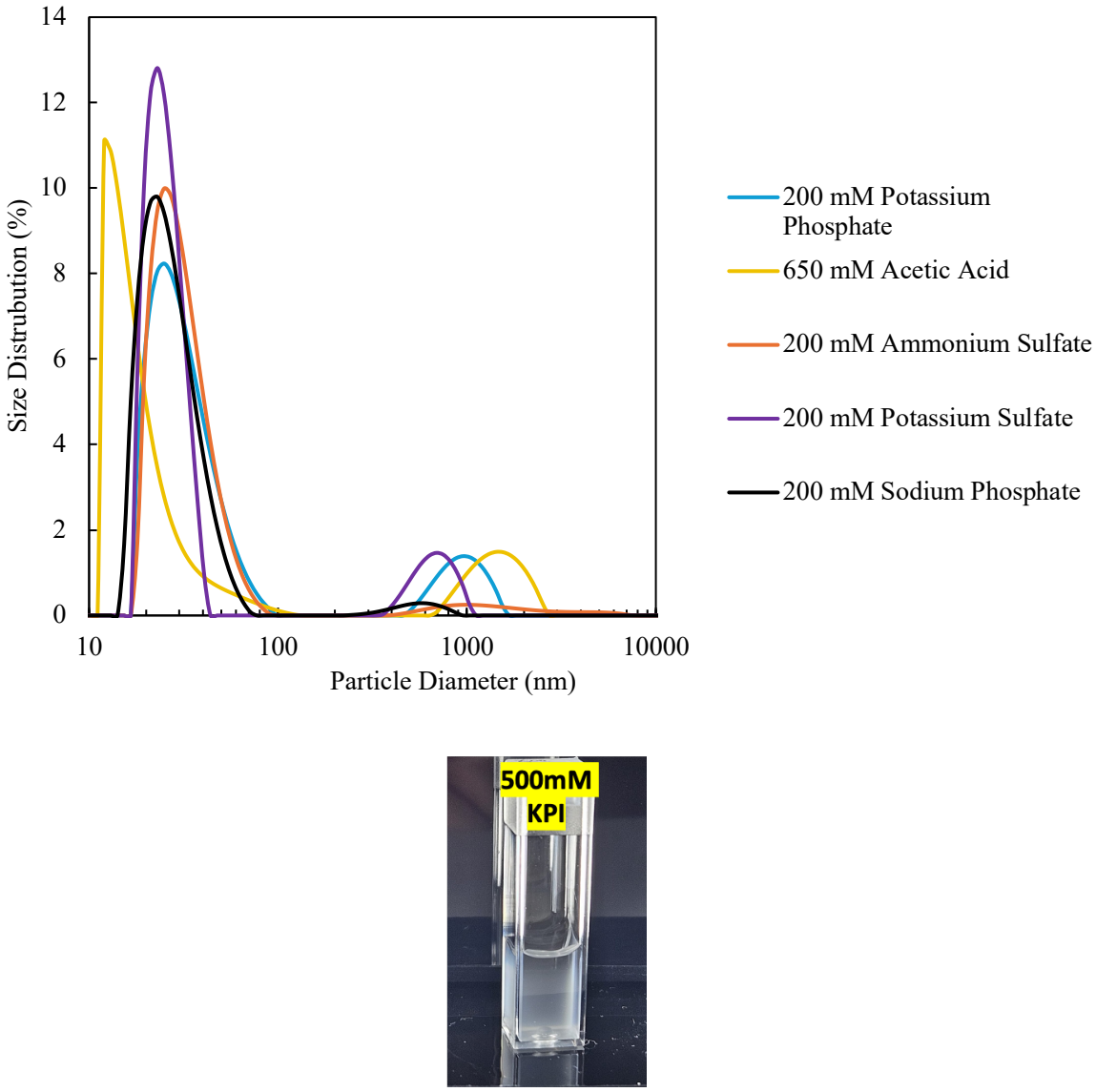

Figure S2: (Top) Representative size distribution (volume weighted) of silk fibroin assembly diameters measured by DLS. Sizes below 200 nm are considered the small, active assemblies that participate in coating formation; sizes above 200 nm are considered large, inactive aggregates that do not participate in coating formation. (Bottom) Photograph of silk fibroin dissolved in 500 mM potassium phosphate solution (pH 5), which is highly turbid due to the presence of micron-scale aggregates.

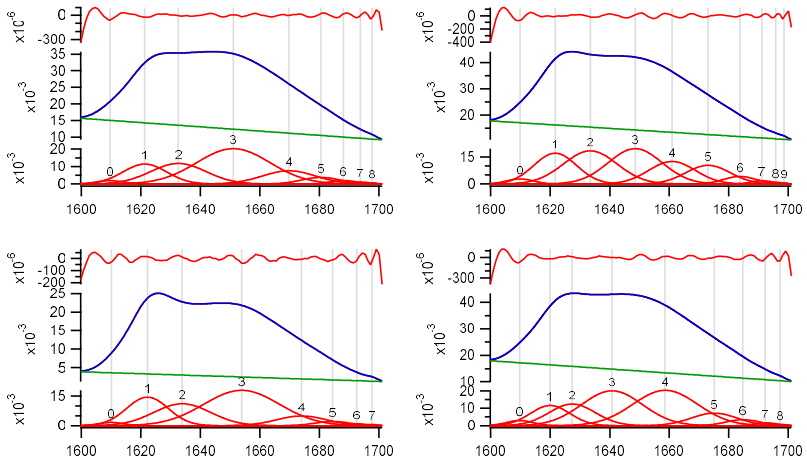

Figure S3: Deconvolution results and fits of ATR-FTIR spectra for solution-phase silk fibroin. Solution conditions are 200 mM phosphate, pH 5, 0.5 mg/mL silk fibroin. Each graph corresponds to one trial for each listed timepoint. TOP: residuals for model fit; MIDDLE: Raw spectra (red) and reproduced spectra from deconvolution (blue); BOTTOM: fitted peaks during deconvolution calculation used for secondary structure assignments.

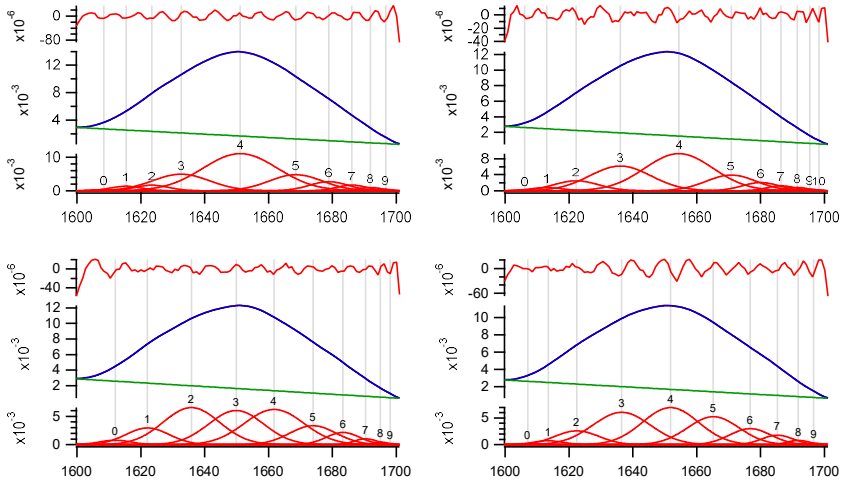

Figure S4: Deconvolution results and fits of ATR-FTIR spectra for solution-phase silk fibroin. Solution conditions are 200 mM ammonium sulfate, pH 5, 0.5 mg/mL silk fibroin. Each graph corresponds to one trial for each listed timepoint. TOP: residuals for model fit; MIDDLE: Raw spectra (red) and reproduced spectra from deconvolution (blue); BOTTOM: fitted peaks during deconvolution calculation used for secondary structure assignments.

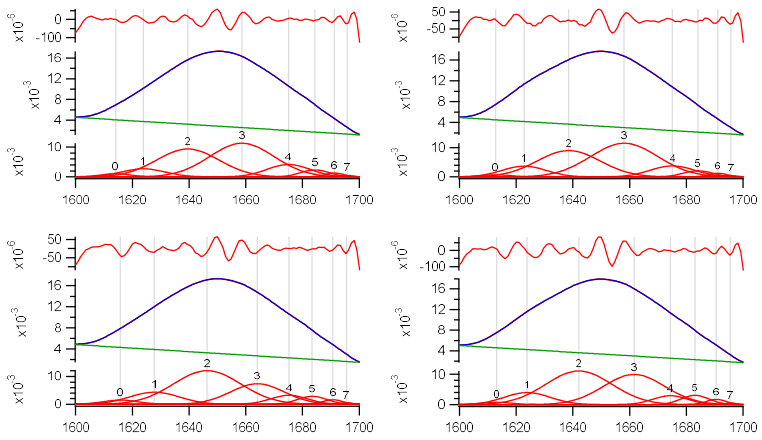

Figure S5: Deconvolution results and fits of ATR-FTIR spectra for solution-phase silk fibroin. Solution conditions are 650 mM acetic acid buffer, pH 5, 0.5 mg/mL silk fibroin. Each graph corresponds to one trial for each listed timepoint. TOP: residuals for model fit; MIDDLE: Raw spectra (red) and reproduced spectra from deconvolution (blue); BOTTOM: fitted peaks during deconvolution calculation used for secondary structure assignments.

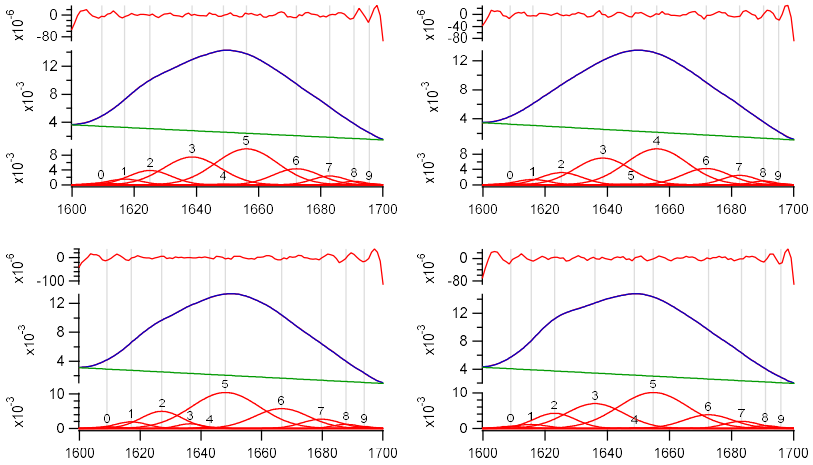

Figure S6: Deconvolution results and fits of ATR-FTIR spectra for solution-phase silk fibroin. Solution conditions are 200 mM potassium sulfate, pH 5, 0.5 mg/mL silk fibroin. Each graph corresponds to one trial for each listed timepoint. TOP: residuals for model fit; MIDDLE: Raw spectra (red) and reproduced spectra from deconvolution (blue); BOTTOM: fitted peaks during deconvolution calculation used for secondary structure assignments.

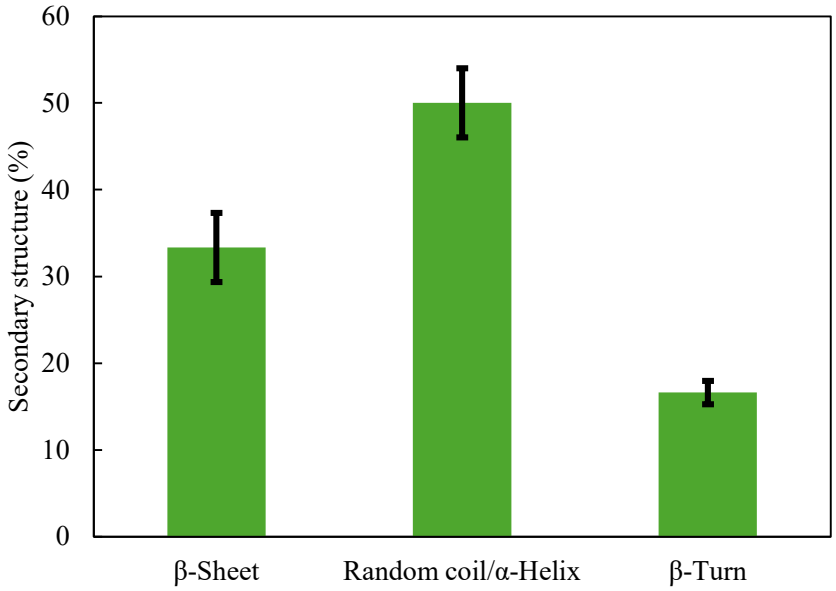

Figure S7: Overall secondary structure content of solution-phase silk fibroin in 200 mM sodium phosphate (solution pH 5, 0.5 mg/mL silk fibroin) ± standard deviation. Sodium phosphate promotes β-sheet content nearly identical to potassium phosphate.

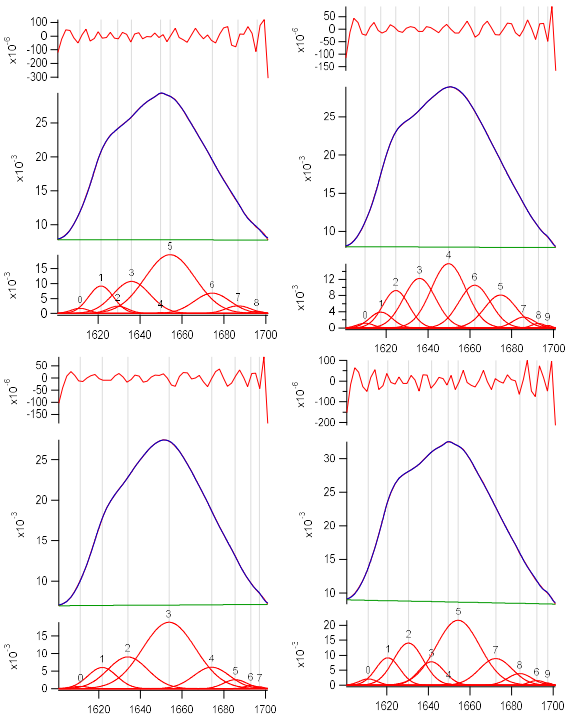

Figure S8: Deconvolution results and fits of ATR-FTIR spectra for solution-phase silk fibroin. Solution conditions are 200 mM sodium phosphate, pH 5, 0.5 mg/mL silk fibroin. Each graph corresponds to one trial for each listed timepoint. TOP: residuals for model fit; MIDDLE: Raw spectra (red) and reproduced spectra from deconvolution (blue); BOTTOM: fitted peaks during deconvolution calculation used for secondary structure assignments.

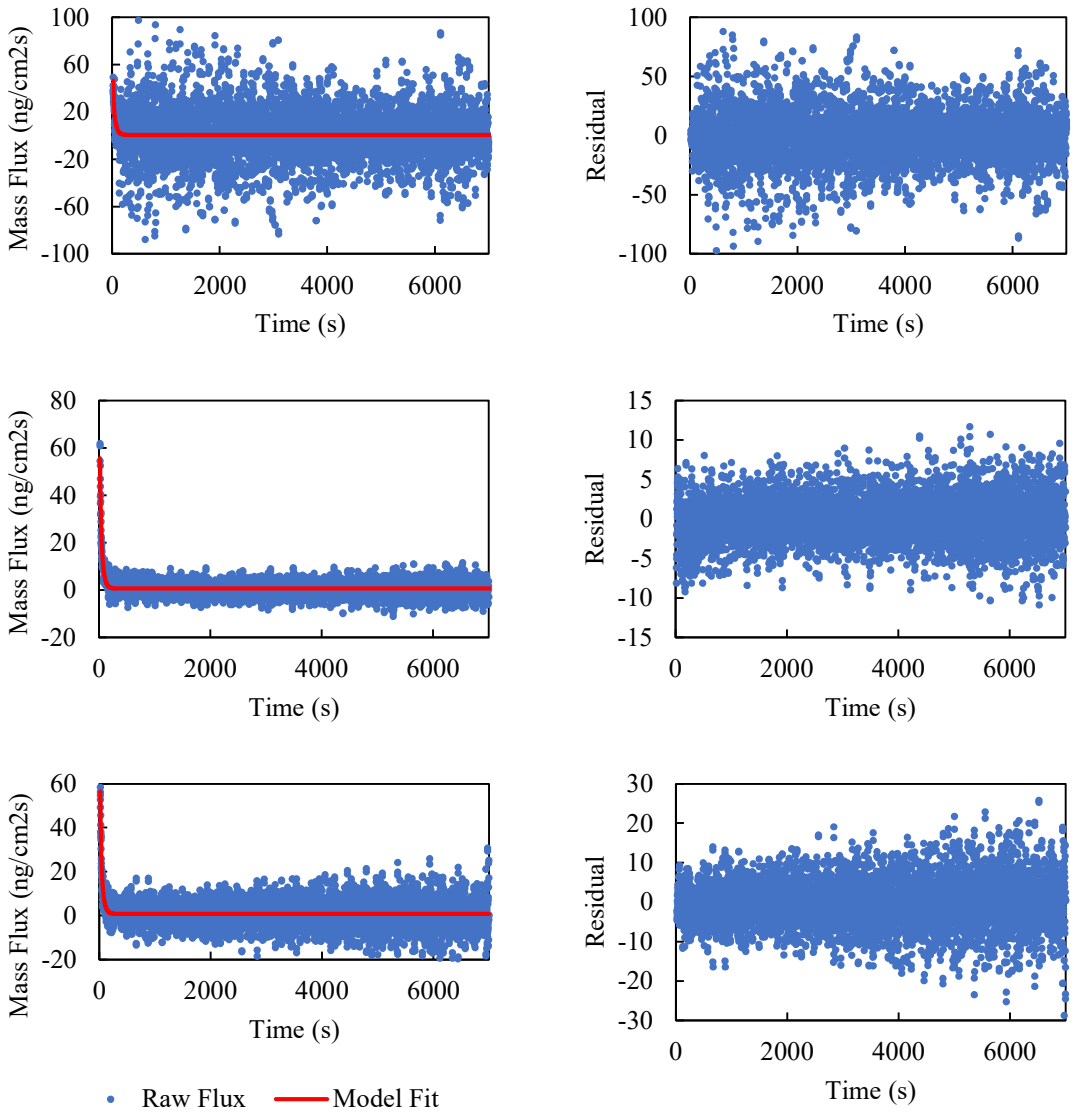

Figure S9: [Left] Two-stage interfacial assembly model (red) fit to mass flux to the surface calculated from QCM-D data (blue). Solution conditions 200 mM ammonium sulfate, pH 5, 0.5 mg/mL. [Right] Residuals of the two-stage interfacial assembly model fit.

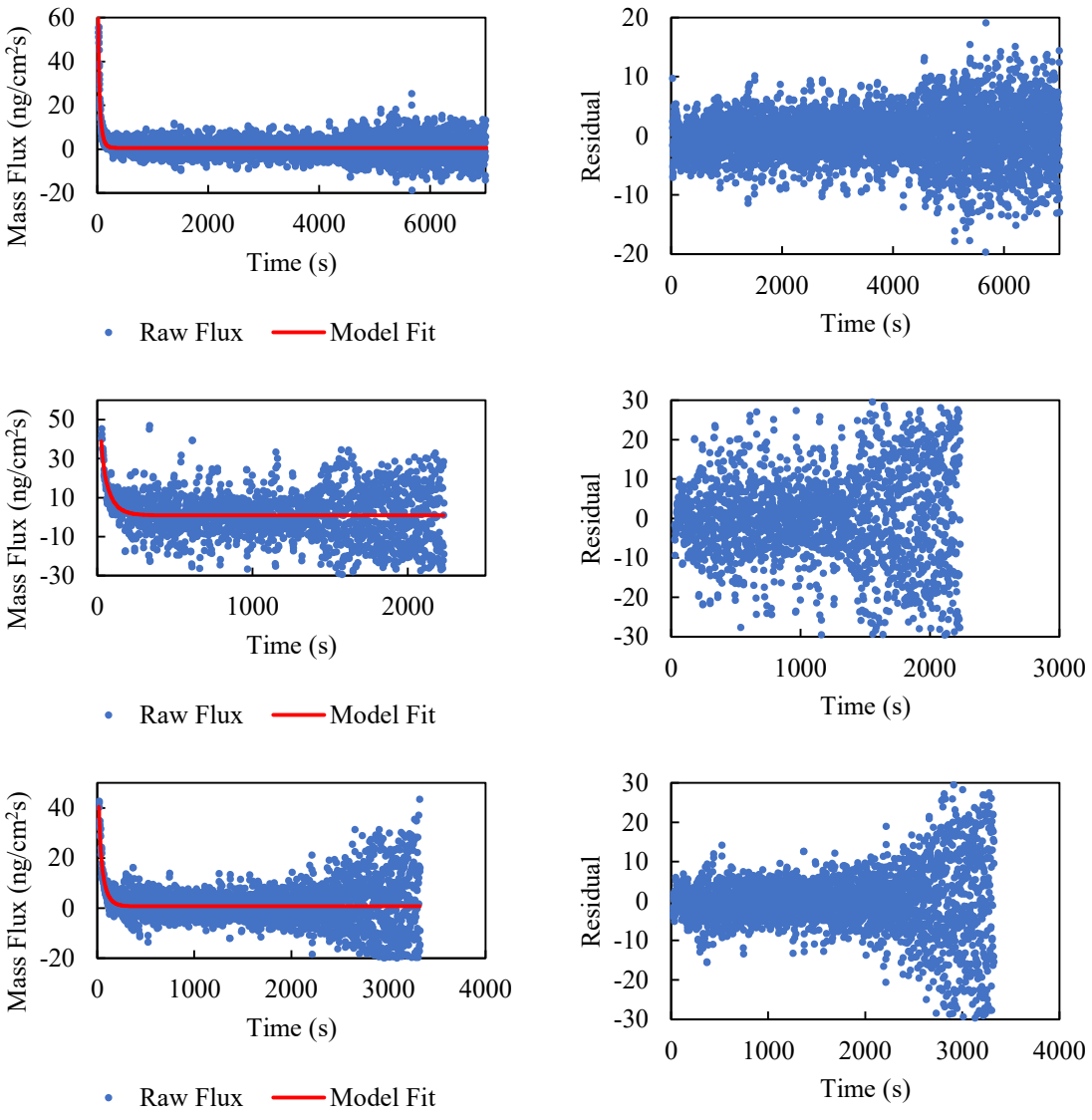

Figure S10: [Left] Two-stage interfacial assembly model (red) fit to mass flux to the surface calculated from QCM-D data (blue). Solution conditions 200 mM potassium sulfate, pH 5, 0.5 mg/mL. [Right] Residuals of the two-stage interfacial assembly model fit.

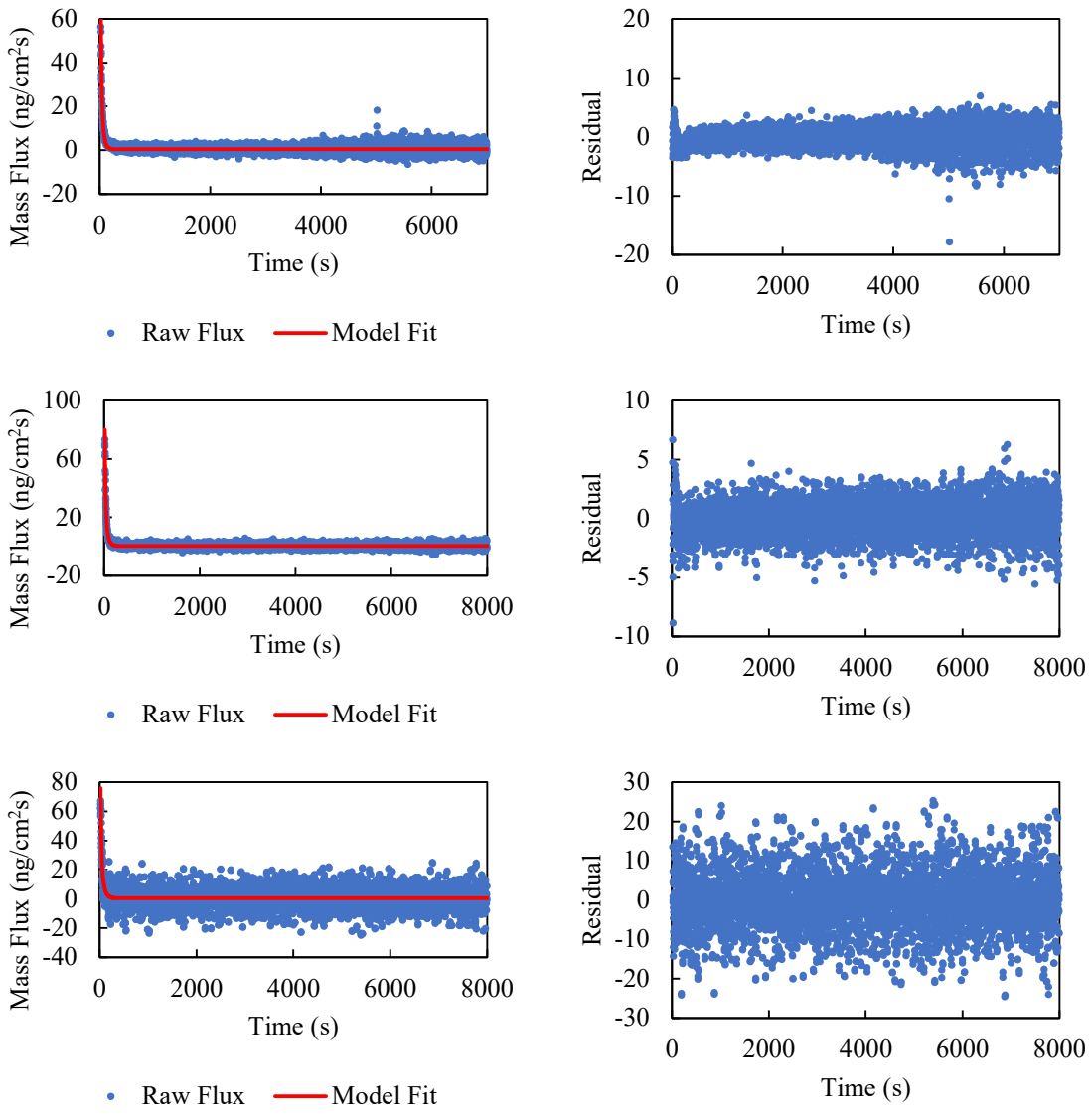

Figure S11: [Left] Two-stage interfacial assembly model (red) fit to mass flux to the surface calculated from QCM-D data (blue). Solution conditions 650 mM acetic acid buffer, pH 5, 0.5 mg/mL. [Right] Residuals of the two-stage interfacial assembly model fit.

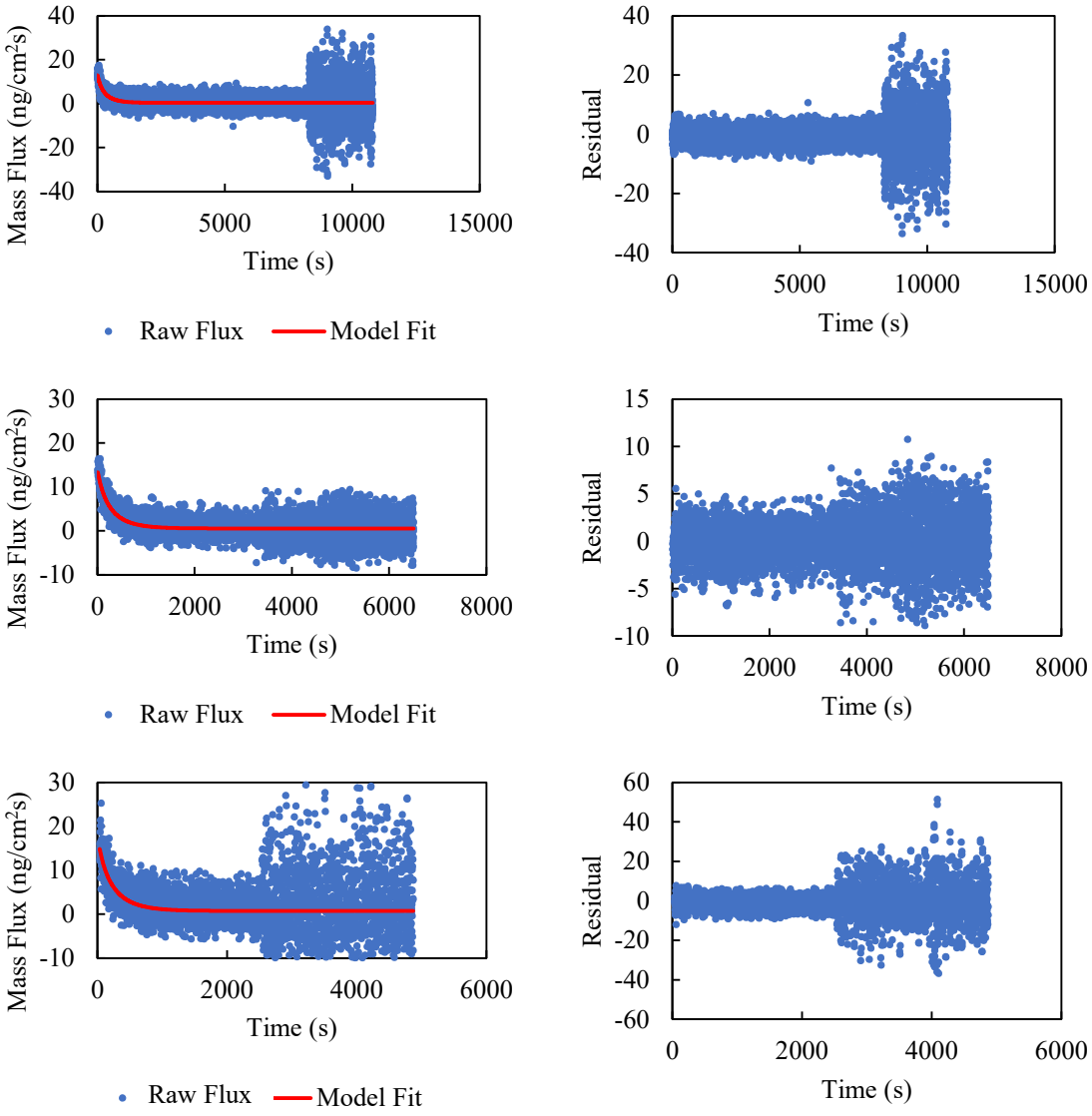

Figure S12: [Left] Two-stage interfacial assembly model (red) fit to mass flux to the surface calculated from QCM-D data (blue). Solution conditions 200 mM potassium phosphate, pH 5, 0.5 mg/mL. [Right] Residuals of the two-stage interfacial assembly model fit.

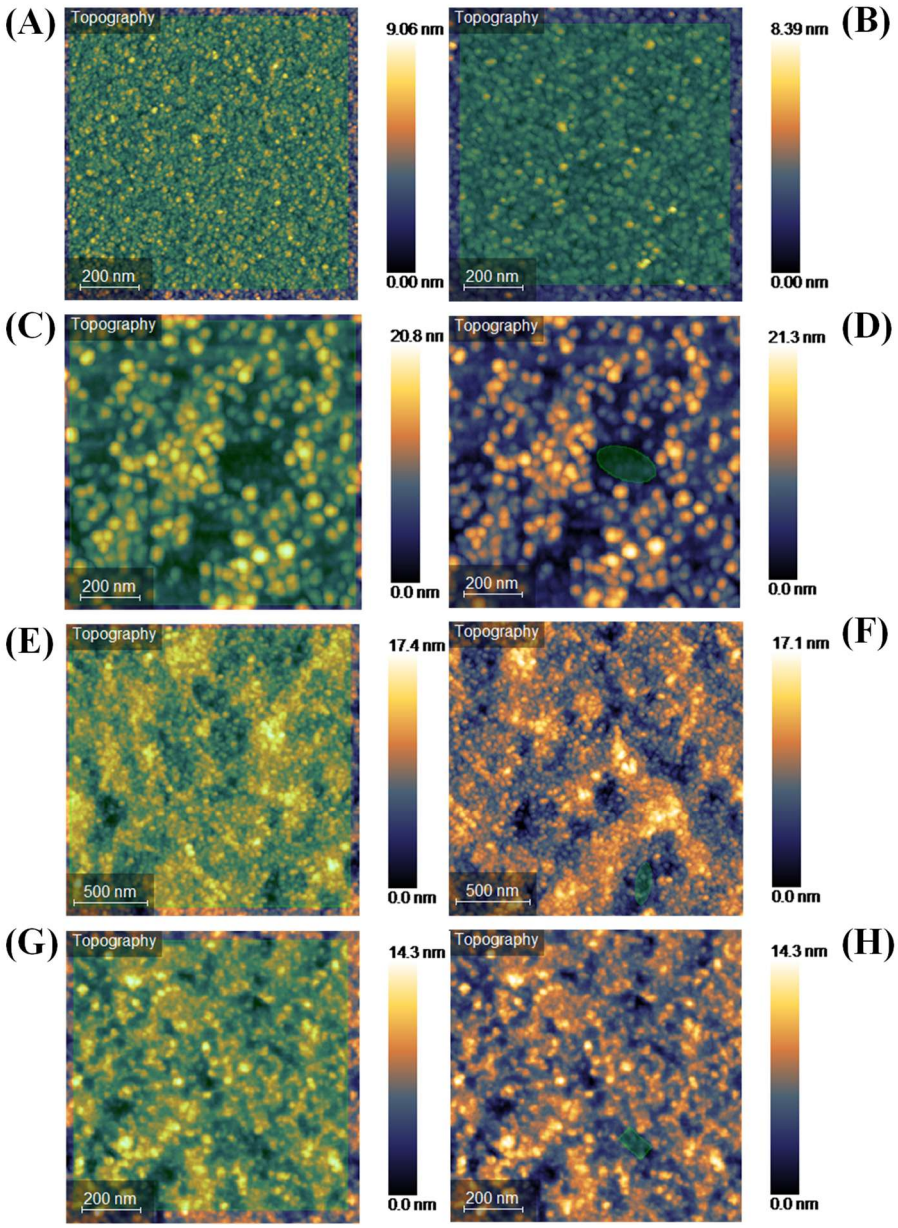

Figure S13: AFM height images of (A) bare TiO2 and silk fibroin coatings formed for 24 hours in (B) 200 mM potassium phosphate, (C & D) 200 mM ammonium sulfate, (E & F) 650 mM acetic acid buffer, (G & H) 200 mM potassium sulfate. Other solution conditions are pH 5 and 0.5 mg/mL silk fibroin. Green masks are the areas used for RMS surface roughness calculation of full coating area (left) and potential exposed substrate areas (right).

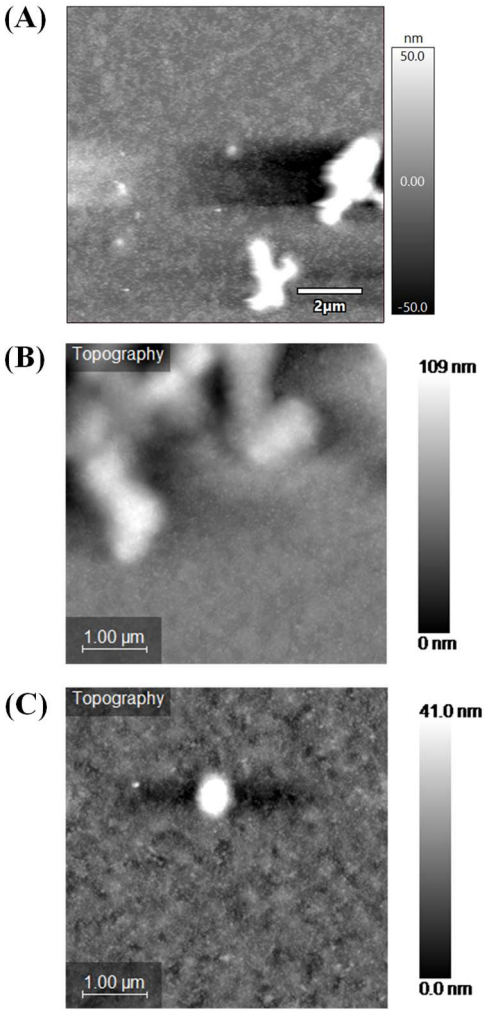

Figure S14: AFM height images of silk fibroin coatings formed for 24 hours in (A) 200 mM ammonium sulfate, (B) 200 mM potassium sulfate, and (C) 650 mM acetic acid buffer. Other solution conditions are pH 5 and 0.5 mg/mL silk fibroin. Images show large surface aggregates formed during the coating process. These large aggregates consist of smaller protein assemblies. No examples of large surface aggregates for coatings formed in potassium phosphate could be found.

References

(1) Wigham, C.; Fink, T. D.; Sorci, M.; O'Reilly, P.; Park, S.; Kim, J.; Zha, R. H. Phosphate-Driven Interfacial Self-Assembly of Silk Fibroin for Continuous Non-Covalent Growth of Nanothin Defect-Free Coatings. **2024**. https://doi.org/10.21203/rs.3.rs-4360925/v1.